Engineering Structures 214 (2020) 110563

Contents lists available at ScienceDirect

Engineering Structures

journal homepage: www.elsevier.com/locate/engstruct

Z-type shear connector for interface of hollow-core slab and cast-in-place topping concrete

E. Yuksel[a,*], A. Gullu[b], Y. Durgun[a], E. Binbir[c], E. Senol[c], A. Khajehdehi[c], H. Saruhan[a]

[a] Istanbul Technical University, Faculty of Civil Engineering, Maslak, Istanbul, Turkey
[b] Istanbul Gedik University, Faculty of Engineering, Kartal, Istanbul, Turkey
[c] Istanbul Technical University, Graduate School of Science, Engineering and Technology, Maslak, Istanbul, Turkey

ARTICLE INFO

Keywords:
Precast hollow-core slab
Topping concrete
Interface shear strength
Bonding

ABSTRACT

Precast hollow-core slabs (*PHSs*) are widely used in precast construction due to their relatively low dead weight and easy assemblage. Cast-in-place topping concrete (*TC*) is utilized to obtain composite sections and to enhance in-plane stiffness of the slab system. Shear transfer between the layers of a composite slab can be provided by the upper face roughness of *PHS*. However, the roughening process may not be preferred in some plants. This paper evaluates the efficiency of Z-type shear connectors applied in the interface between *PHS* and *TC*. Three dissimilar interface conditions (i.e., Z-reinforced, smooth and rough) were studied experimentally in full-scale specimens. Push-off loading was applied to evaluate the interface shear transfer capability of the specimens, and Z-type shear connectors were found to be the most effective when they are applied at each joint between *PHSs*. The achievements of some code equations to assess interface shear strength were also investigated, and an alteration for the interface shear capacity equation of ACI 318M is proposed.

1. Introduction

Precast/pre-stressed hollow-core slabs (*PHSs*) are widely used in precast constructions due to their advantages, including easy assemblage and low self-weight/live load ratio [17]. Cast-in-place topping concrete (*TC*) is often applied to obtain a smooth finish. Partial or fully composite action is supplied by different interaction details, such as interface shear, properly anchored ties or both, and enables horizontal shear force transmission between the segments of composite sections.

Scott [20] performed bi-directional tests on machine-made hollow-core slabs with depths of 20 cm and widths of 60 cm. The study compared the experimental results with the equations defined in design codes and found that the ultimate flexural capacity of *PHS* can be precisely predicted.

Ueda and Stitmannaithum [21] predicted shear strength of *PHS* by considering the crack pattern. Although web shear cracking strength was computed through the conventional elastic analysis method, flexural-shear cracking strength was obtained by their proposed approach.

Yang [22] suggested a design procedure to determine shear capacity of *PHS* webs and verified their proposed equation with finite element models and two test specimens. The procedure accounts for diverse loading cases, prestress levels, types of cross-section, material and geometric parameters.

Loove and Patnaik [13] proposed a parabolic equation to evaluate horizontal shear stress in composite concrete beams. After testing 16 beam specimens, they mentioned that an as-cast surface with coarse aggregate could have adequate horizontal shear strength, and stirrups were ineffective until horizontal shear stress exceeded some specific values.

Pajari and Koukkari [15] performed 10 large scale tests on *PHSs* supported on beams. The failure mode was web-shear for all specimens. The shear resistance of *PHSs* was considerably reduced due to deflection of the supporting beams. It was also declared that the interaction between the slab and beam was an important factor affecting the shear resistance. Pajari [16] proposed a simple calculation model based on the experimental results.

Julio et al. [12] conducted an experimental study to investigate the interface shear strength between two concrete layers. Different techniques were considered to increase surface roughness, and the highest interface shear strength was obtained from the sand-blasting technique. In addition, pre-wetting was found to be insignificant in terms of affecting interface shear strength.

Girhammar and Pajari [10] conducted an experimental and theoretical study on the effect of structural toppings on the shear capacity of hollow core slabs. They also evaluated the adequacy of bond strength of the non-treated interface. They reduced thickness of *PHSs* by increasing

* Corresponding author.
E-mail address: yukselerc@itu.edu.tr (E. Yuksel).

https://doi.org/10.1016/j.engstruct.2020.110563
Received 31 August 2019; Received in revised form 3 February 2020; Accepted 21 March 2020
Available online 20 April 2020

Nomenclature

Variables

A_{cv}	concrete shear transfer area
A_{eff}	effective shear area
$A_{section}$	sectional area
A_{vf}	shear reinforcement area
$A_{v,\min}$	minimum horizontal shear reinforcement area
b	slab width
b_w	web width of cross section
b_{wi}	width of interface
c	cohesion coefficient
d	distance from extreme compression fiber to centroid of longitudinal tension reinforcement
f_c	concrete compressive strength
f_{ct}	concrete tension strength
f_y	steel yield strength
h	slab thickness
h_g	center of gravity from bottom
I	moment of inertia
I_{comp}	moment of inertia of composite section
L	span length
N	normal force on interface
s	center-to-center spacing of the shear reinforcements
t_{cover}	cover concrete for strands
T	shear force
T_i	interface shear force
Q	first moment of inertia
V_r	interface shear force
V_{Rdi}	interface shear force
α	angle between shear reinforcement and shear plane
μ	friction coefficient
ν	strength reduction factor
ρ	shear reinforcement ratio
σ_n	compressive stress on the interface
τ_h	interface shear stress

TC thickness without allowing for decrements in load carrying capacity. They concluded that *TC* may increase shear capacity by up to 35%.

Ajdukiewicz et al. [3] performed experiments on *PHSs* with typical concrete toppings. No interface reinforcement or any special preparation process was used at the interface. Experimental results displayed that the interaction between the segments of composite section was quite efficient till 95% of the ultimate load capacity.

Santos and Julio [19] presented a detailed review of the design expressions for the interface shear strength of *PHSs*. They compared the existing equations and concluded that roughness of concrete substrate is a key parameter.

Mones and Brena [14] performed push-off tests on two different types of *PHSs*—namely, dry and wet mixes. In total, 24 specimens were tested to determine the interface shear capacity, and no interface shear reinforcement was applied. The interfacial shear stresses were found to be related to surface roughness, sandblasting for wet-mix specimens and grouting.

Adawi et al. [2] experimentally investigated the effect of *TC* on the behavior of *PHSs*, aiming to evaluate North American design standards. The tested specimens showed a better performance than the limit suggested by the standards.

Baran [5] investigated flexural behavior of *PHSs* with cast-in-place *TC*. The specimens did not have a specially prescribed roughness or shear reinforcement detail. The flexural capacities obtained from the numerical and experimental studies were compared. A full composite action was obtained until the first cracking, and cracking moment and initial stiffness were improved by the contribution of *TC*. Nevertheless, the ultimate moment capacity of the slabs was barely affected by the existence of *TC*.

Ibrahim et al. [11] performed shear type tests on *PHSs* with *TC*. The effects of two roughness types (i.e., smooth and roughened) and three mixture types (i.e., wet, ponded and dry) were evaluated. It was found that surface roughness and moisture were not related with the obtained failure modes. The roughened surface was found to be more effective to maintain the interaction between *PHS* and *TC*. The wet specimens in the two groups had higher load-carrying capacity.

Bernardi et al. [6] proposed a general design method to predict load distribution at serviceability conditions for *PHSs* with *TC*. Each panel was considered as Saint-Venant beams connected to other ones via rotational springs. Hence, the unique unknown of the system was reduced to the shear forces transferred along the structural joints. The model was verified with the experimental results existing in the literature and code provisions. They stated that the proposed procedure can be used for design purposes.

This paper experimentally evaluates the effectiveness of Z-type shear connectors. The performances of 10 full-scale specimens with distinct interface types (i.e., Z-reinforced, smooth and roughened) were compared. The specimens with three-rows of Z-type connector and the roughened interfaces satisfied the full composite actions.

2. Experimental study

Two *PHSs* were combined to make each specimen. The thickness of *PHSs* and cast-in-place *TC* were 150 and 70 mm, respectively, and plan dimensions of the specimens were 2 × 1.2 = 2.4 m and 6.0 m. A characteristic cross-section of the specimens is presented in Fig. 1. Sectional characteristics of the specimens for pre- and post-composite action are listed in Table 1 as well.

The production steps of the slab system that is similar to the practice are as follows: (i) Cleaning and pre-wetting of the longitudinal joints between adjacent *PHSs* [12,14,11], (ii) Filling the joints with non-

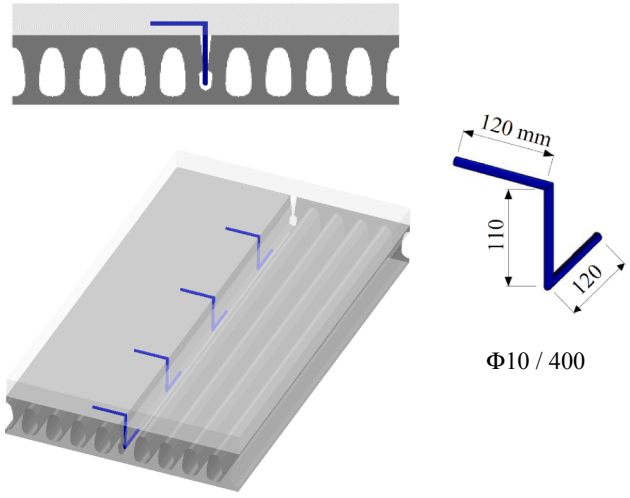

Fig. 1. Typical cross-section of the specimens and Z-type shear connector.

Table 1
Cross-sectional properties of the specimens (for single *PHS*).

Property		PHS	Composite section
		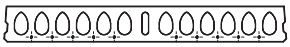	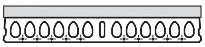
Slab thickness (mm)	h	150	220
Slab width (mm)	b	1200	1200
Slab web width (mm)	b_w	300	300
Sectional area (mm^2)	$A_{section}$	123.6×10^3	207.6×10^3
Center of gravity from bottom (mm)	h_g	75.04	119.53
Moment of inertia (mm^4)	I	3.033×10^8	9.424×10^8
First moment of inertia (mm^3)	Q	–	5.499×10^6
Cover concrete for strands (mm)	t_{cover}	20	20

Table 2
Definition of the specimens.

Tag	Interface	Test Type
Z1F-1 Z2F-1	One-row Z-reinforcement and smooth	Flexural
R1F R2F	Roughened	Flexural
S1F S2F	Smooth	Flexural
Z1S-1 Z2S-1	One-row Z-reinforcement and smooth	Shear
Z1S-3 Z2S-3	Three rows Z-reinforcement and smooth	Shear

shrinkage grout, (iii) Placement of Z-type shear connectors in the joints (see Fig. 1) with specific intervals, (iv) Setting up wood formworks at slab edges, (v) Placement of wire mesh (188 mm^2/m in both direction) and (vi) Casting of *TC*.

The specimens were designed according to ACI 318M. Span lengths (L) and dead and live loads were taken as 5.6 m, 4.76 kN/m^2, and 12.00 kN/m^2, respectively.

Three distinct interface cases were studied. The definitions of specimens and their tags are listed in Table 2. Construction stages and interface profiles of the specimens are revealed in Fig. 2. The depth of the roughness was 6 mm in R1F and R2F according to ACI 318M (Fig. 2c). Diameter of the Z-type shear connectors was 10 mm, and they were placed in the longitudinal joint between *PHSs* with 400-mm intervals in Z1F-1, Z2F-1, Z1S-1, Z2S-1, Z1S-3 and Z2S-3 (Fig. 2a, d and e). Nominal yield strength of Z connectors was 420 MPa. The additional

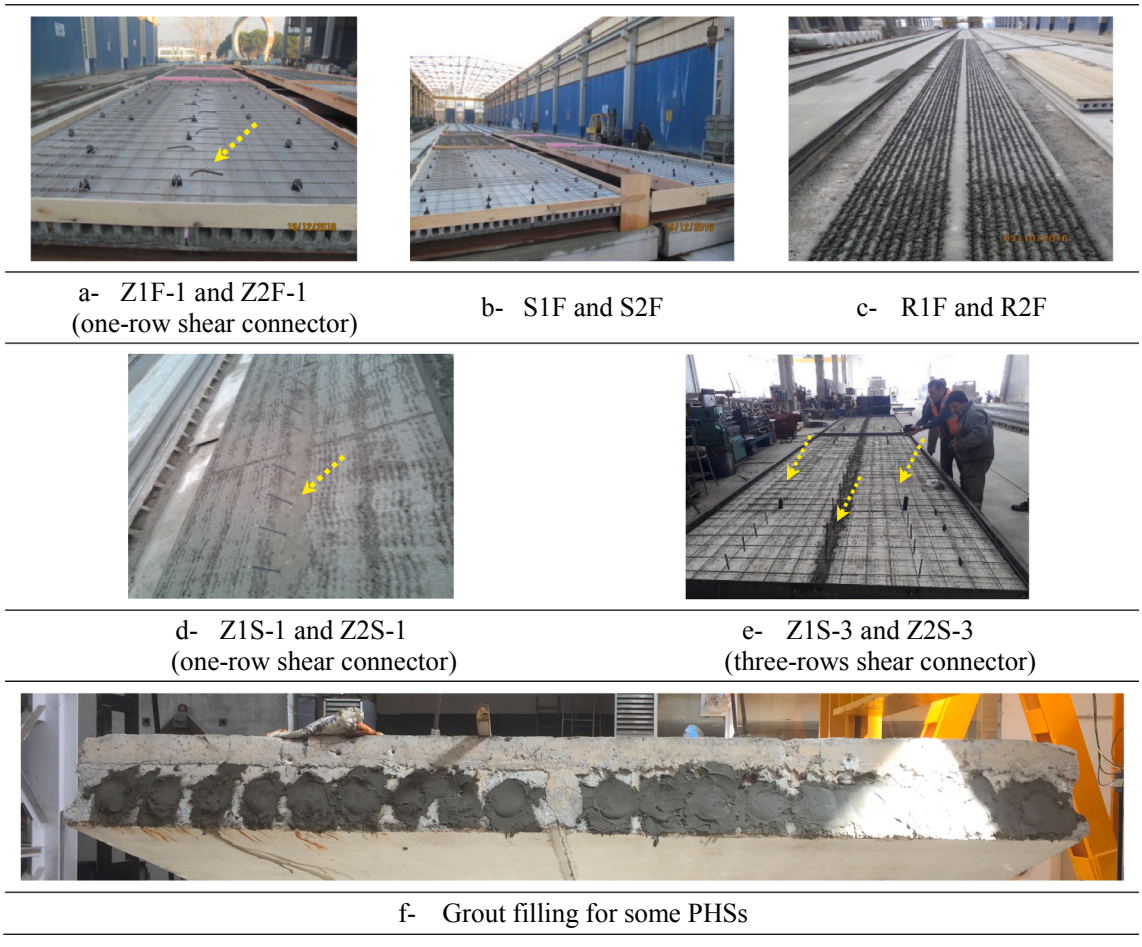

Fig. 2. Interface details of the specimens and the grout filling.

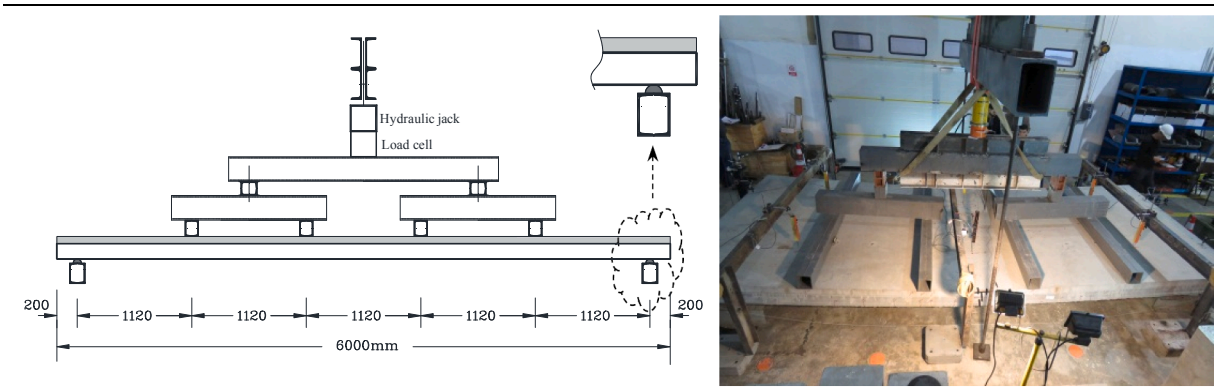

a- Flexural tests

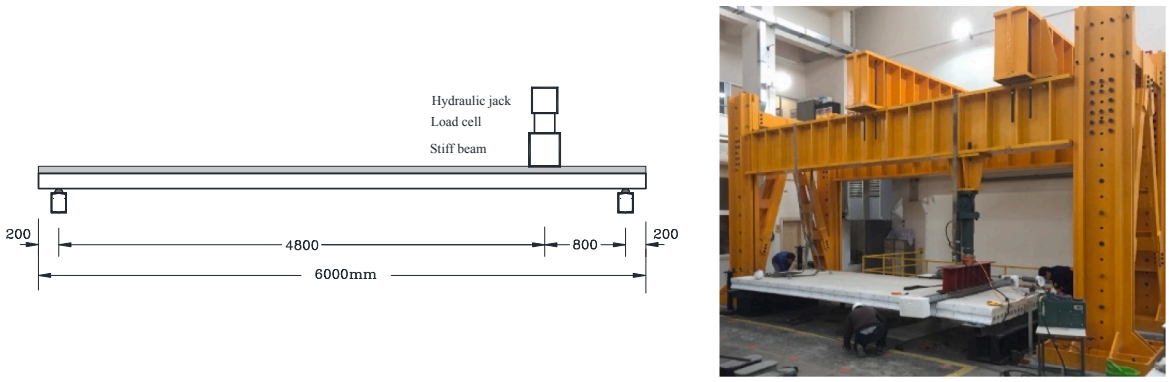

b- Shear tests

Fig. 3. Testing set-ups.

Z-type connectors were placed in the broken and grouted holes of Z1S-3 and Z2S-3 at their ends in 2.0 m lengths, Fig. 2e. Z1S-3 and Z2S-3 represent the practice in which Z-type connectors are placed at each longitudinal joint between the adjacent *PHSs*. However, Z1S-1 and Z2S-1 were tested to evaluate the effect of the shear reinforcement area on the composite action.

The concrete compressive strengths in 28 days were 44.5, 44.3 and 42.6 MPa for *PHS*, *TC* and grout mortar, respectively, and nominal yield strengths of the steels were 1860 MPa and 500 MPa for prestressing strand and wire mesh, respectively.

PHSs of the specimens were pretensioned with ten 7-wire strands having 3/8″ diameter, see Fig. 1. The strands were pretensioned to 65% of their nominal yield strength.

Six of ten specimens (Z1F-1, Z2F-1, S1F, S2F, R1F, R2F) were utilized for flexural tests, while the remaining (Z1S-1, Z2S-1, Z1S-3, Z2S-3) were used in the shear tests. Before the shear tests, voids of *PHSs* were filled with grout at one end (2 m in width) to increase the sectional shear capacity (Fig. 2f).

Two independent testing set-ups were used for the flexural and shear tests. The specimens were simply supported. In the flexural tests, four concentric forces placed with equal distances in the span were applied to the specimens with steel beams placed on rubber pads (Fig. 3a). In the shear tests, one stiff steel beam placed on rubber pad was positioned 800 mm away from the support (Fig. 3b) to achieve a shear dominant behavior.

Slow-rate load increments were applied to the specimens. One load cell was used to measure the load, and several *LVDTs* were utilized in various positions of the specimens to measure absolute and relative displacements. The relative vertical and horizontal displacements between *PHSs* and *TC* were measured at four discrete sections on both edges of the specimens. Six strain gauges were adhered to the lower and upper flanges of the *PHSs* and *TC* at the loading section to measure longitudinal strains (Fig. 4).

No separations were observed between *PHSs* and *TC* when the specimens were arrived to the laboratory. During the waiting phase in the laboratory, some corner separations of *TC* were observed for S1F, S2F, Z1F-1 and Z2F-1 because of shrinkage (Fig. 5a–b). It was expected for smooth interfaces of S1F and S2F. For Z1F-1 and Z2F-1, possible reason for the separation was that the effectiveness of Z-type connectors decreases away from the joint. No such evidence was observed for the three rows of Z-type connectors and the roughened specimens (Fig. 5c–d).

The full-scale test specimens may have the following drawbacks compared with the real world:

(i) Though continuity exists in the transversal direction due to *TC*, the specimens consist of only two *PHSs*.
(ii) Though continuity exists in the longitudinal direction due to *TC* and the wet connection of supporting beam, the specimens were simply supported elements.

a- Relative up-lift and slippage measurements at the interface

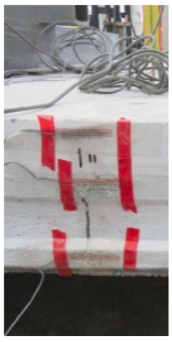

b- Longitudinal strain measurements

c- The displacement transducers

Fig. 4. The measuring system.

3. Test results

3.1. Load-displacement relationships

Mid-span displacement vs. load relations are presented in Fig. 6, although displacements of the specimens were measured at *L/4* intervals. The responses of two *PHSs* are presented together in the graphics. Almost identical responses were obtained from twin *PHSs*. The flexural and shear test results are compared in Fig. 7.

In the flexural tests, the first crack was observed at approximately 180 kN for all specimens. Z-type shear connectors supplied partial hardening after first cracking. The maximum force was 300 kN for S1F, S2F, Z1F-1 and Z2F-1 specimens, whereas it was 450 kN for the roughened specimens. The initial stiffnesses of all specimens were almost identical prior to the first cracks (Fig. 7a), and the maximum mid-span displacement was approximately 260 mm (*L*/21). Experiments were stopped there for the crack widths increased extremely and some possible safety issues of the testing setup. Full composite action was obtained prior of the first cracking for S1F and S2F similar to the Baran's conclusion [5], the hardening loss point for Z1F-1 and Z2F-1. Full composite action was achieved throughout the tests of R1F and R2F.

Loss of contact between *PHS* and *TC* was observed about 60% of the ultimate load carrying capacity as well as 10% of the ultimate displacement capacity for S1F and S2F. These observations are contradicting with the findings of Ajdukiewicz et al. [3] that declared an as-cast surfaces are quite efficient till 95% of the ultimate load. The results obtained for R1F and R2F are totally agree with the conclusion of Santos and Julio [19] who state that roughness of the interface surface is quite effective on the composite behavior.

In the shear tests, first cracking was recorded between 280 and 320 kN for the specimens (Fig. 7b). However, maximum strengths were obtained as 400 and 500 kN for Z1S-1 and Z1S-3, respectively. Moreover, Z1S-3 and Z2S-3 responded with more stability in the plastic range.

3.2. Relative displacements between PHSs and TC

The horizontal (slippage) and vertical (debonding) relative displacements between the *PHSs* and *TC* were measured and are analyzed in this section. Slippage initiated in the early stages of S1F and S2F tests. Slope of the load displacement curve was significantly altered after the first cracking (Fig. 8), and the maximum slippage observed was under 16 mm in S2F. For Z1F-1 and Z2F-1, slippage occurred after approximately 240 kN and 210 kN, respectively (Fig. 8). Slippage increased gradually by the increment of vertical displacements, and no slippage was observed for the roughened specimens (R1F and R2F) and specimens of Z1S-3 and Z2S-3 (Fig. 8). Very limited amount of slippage (about 0.2 mm) was recorded for the other specimens (Z1S-1 and Z2S-1).

a- Z1F-1 and Z1F-2

b- S1F and S2F

c- R1F and R2F

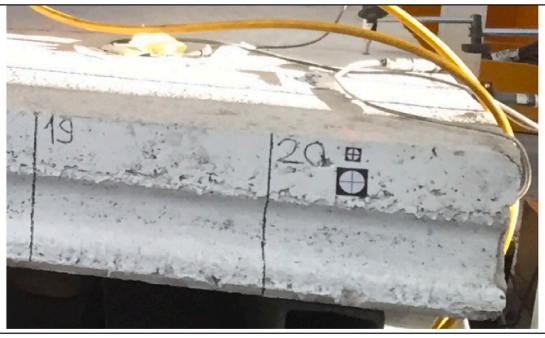

d- Z1S-3 and Z2S-3

Fig. 5. TC separation prior the testing.

Similar trends were observed in terms of debonding. The maximum separation was about 4 mm for S1F, S2F as well as 6 mm for Z1F-1 and Z2F-1. No separation was recorded for R1F and R2F and the shear specimens of Z1S-1, Z2S-1, Z1S-3 and Z2S-3 (Fig. 9).

3.3. Longitudinal strains

Strain gauges adhered to *TC* supplied valuable data throughout the tests. Longitudinal compressive strains vs. load relations are shown in Fig. 10. In the flexural tests, maximum compressive strains at *TC* were 0.04%, 0.13% and 0.28% for smooth, Z-reinforced and roughened specimens, respectively. On the other hand, the strains were 0.10–0.12% for the shear specimens.

3.4. Damage patterns and failure modes

Crack patterns recorded in the flexural tests are depicted in Fig. 11a, b and c. The cracks distributed continuously between the load points, and the maximum crack widths were 1.6 mm, 3.4 mm and 6.0 mm for the smooth (S1F and S2F), Z-reinforced (Z1F-1 and Z2F-1) and roughened (R1F and R2F) specimens, respectively. During the flexural tests, slippage and separation of *TC* were common damage modes for S1F, S2F, Z1F-1 and Z2F-2. The events initiated in earlier steps of the tests and gradually increased (Fig. 12a and b). Conversely, no slippage and separation were observed in R1F and R2F. Web shear cracks, pre-stress loss and joint separation were observed at latest stages of these tests (Fig. 12c).

In the shear tests, although a few flexural cracks were observed at earlier steps, leading damage mode was shear cracking for all specimens (Fig. 11d and e). Web shear cracking, pre-stress loss, joint separation as well as slippage and *TC* separation were not observed in Z1S-3 and Z2S-3 (Fig. 12d and e).

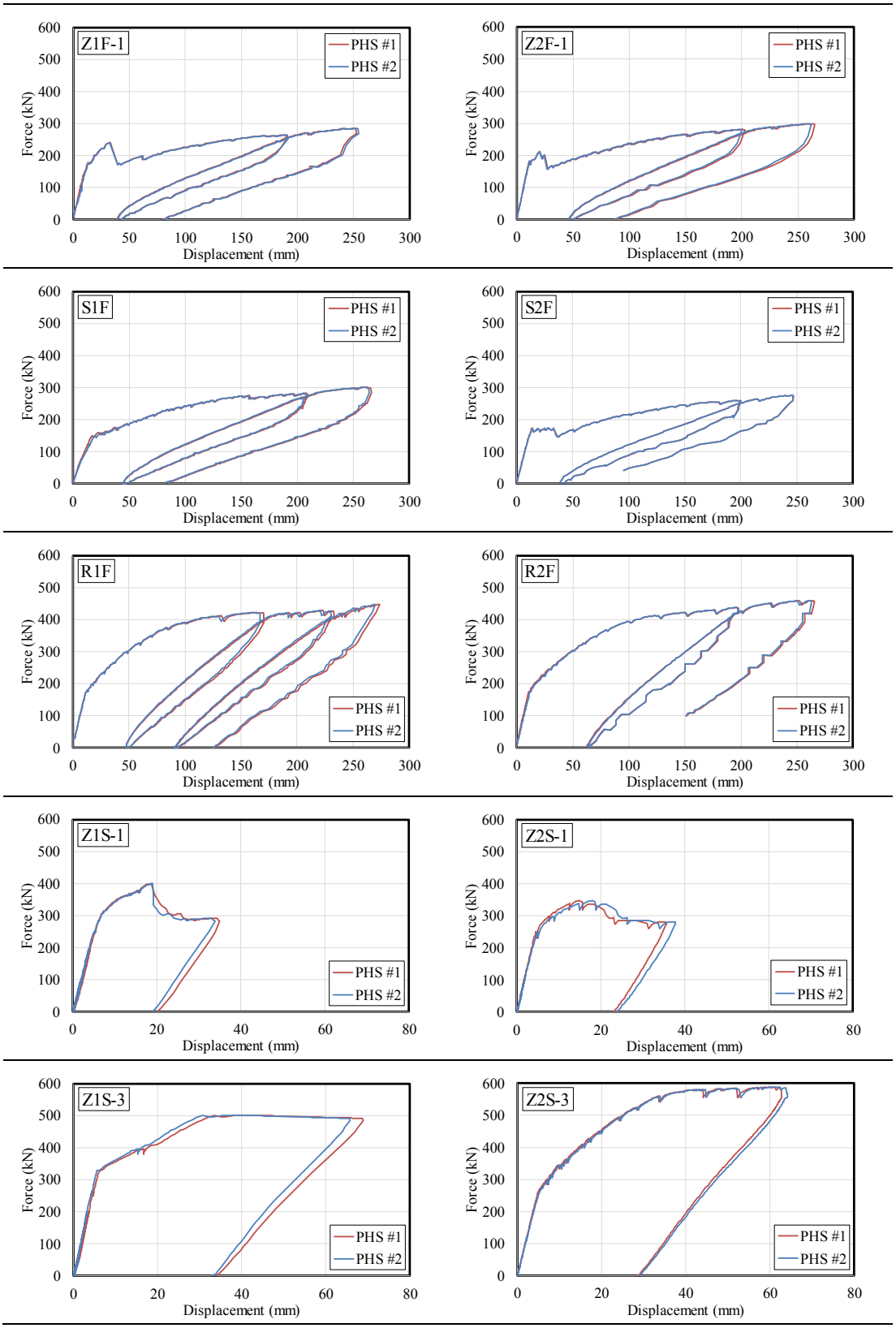

Fig. 6. Force-displacement relationships of the specimens.

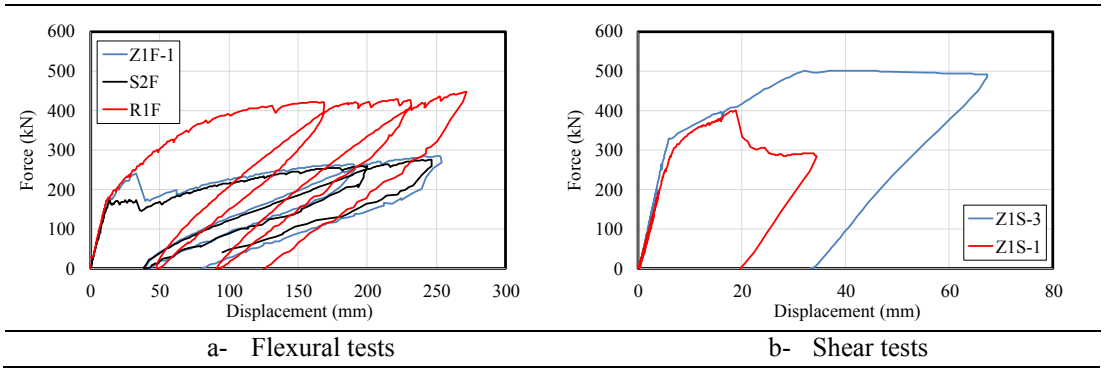

Fig. 7. Comparison of the force-displacement relationships.

3.5. Interface shear stresses

Interface shear stress between the segments of composite slabs were computed by Eq. (1), where τ_h is horizontal shear stress, T is shear force, Q is static moment of cross-sectional area of *TC* with respect to neutral axis of the composite section, I_{comp} is moment of inertia of the composite section and b_{wi} is width of the interface.

$$\tau_h = \frac{T \times Q}{I_{comp} \times b_{wi}} \quad (1)$$

Eq. (1) is valid when full interaction exists between the segments of the slab system. Therefore, the experimental shear stresses were generated prior to separation of *TC* in S1F, S2F, Z1F-1 and Z2F-1 (Fig. 13a). In the flexural tests, the obtained maximum shear stresses were 0.2 MPa, 0.3 MPa and 0.5 MPa for smooth (S1F and S2F), Z-reinforced (Z1F-1 and Z2F-1) and roughened specimens (R1F and R2F), respectively.

In the shear tests, maximum interface shear stresses were obtained as 0.95 MPa and 1.20 MPa for Z-reinforced specimens of Z1S-1 and Z1S-3, respectively (Fig. 13b).

4. Comparison of the test results with the code estimation

The interface shear stress capacity of the slab systems was estimated by different codes in terms of some critical values and equations.

ACI 318M [1] defines some general rules for the composite members. The interface shear force (T_i, [N]) is calculated by an empirical equation (Eq. (2a)), where b_w is web width of cross section [mm], and d [mm] is distance from extreme compression fiber to centroid of longitudinal tension reinforcement. The interface shear stress is calculated by Eq. (2b), where A_{eff} is effective shear area determined from the shear diagram, Fig. 14.

$$T_i\,[N] = 0.55 b_w d \quad (2a)$$

$$\tau_h\,[MPa] = T_i / A_{eff} \quad (2b)$$

If the interface shear force is aimed to transfer by shear reinforcement, ACI 318M requires a minimum horizontal shear reinforcement area ($A_{v,\min}$) as given in Eqs. (3a) and (3b), where b_w is web width [mm], s is the center-to-center spacing of the shear reinforcements [mm], f_c and f_y are compressive strength of concrete and yield strength of shear reinforcement [MPa].

$$A_{v,\min}\,[mm^2/s] = 0.062\sqrt{f_c}\, b_w s / f_y \quad (3a)$$

$$A_{v,\min}\,[mm^2/s] = 0.35 b_w s / f_y \quad (3b)$$

The required shear reinforcement area for the specimens is calculated as 210 mm^2 according to ACI 318 by Eq. (3a) where $f_c = 35$ MPa, $f_y = 420$ MPa, $b_w = 600$ mm and $s = 400$ mm. Z-type shear connector areas of the tested specimens were 236 mm^2 and 79 mm^2 for three-rows and one-row shear connector cases with intervals of 400 mm, respectively. Although fully composite action was observed for three-rows Z-type connector case, loss of interaction was recorded in one-row connector case after hardening loss. Hence, ACI-318 equations could be utilized to determine the required area of Z-type shear connectors.

The various code estimations for the interface shear strength, Table 3, are illustrated on the experimental displacement vs. interface shear stress diagrams where only the fully interacted parts of the tests are shown, Fig. 15.

In the flexural tests, full separation of *TC* was observed after 0.2 MPa interface shear stress for S1F and S2F. Also, partial separation of *TC* was observed after 0.3 MPa interface shear stress at both edges of Z1F-1 and Z2F-1. Full bonding was experienced for R1F and R2F. The maximum interface shear stress reached 0.5 MPa. Although the estimations of ACI 318M for smooth and Z-reinforced specimens were appropriate with the test results, they are relatively conservative for the roughened specimens. The interface shear capacity estimations of CAS are relatively conservative, see Table 3 and Fig. 15. A similar conclusion was made by Adawi et al. [2]. Moreover, CEB-FIP Model Code [9] is quite conservative for the smooth interfaces.

In the shear tests, full bonding was observed for Z1S-3 and Z2S-3. The maximum interface shear stress was 1.2 MPa. Limited separation was observed after interface shear stress of 0.5 MPa and 0.7 MPa at both edges of Z1S-1 and Z2S-1, respectively.

An alteration in Eq. (2a) is advised for the roughened and Z-reinforced at each joint (Z1S-3 and Z2S-3) between *PHS* type systems, as given in Eq. (4). The product of Eq. (4) is also revealed in Fig. 15c and e.

$$T_i\,[N] = 0.75 b_w d \quad (4)$$

5. Conclusions

The efficiency of the Z-type shear connector application was evaluated through the full-scale tests. The results were compared with the

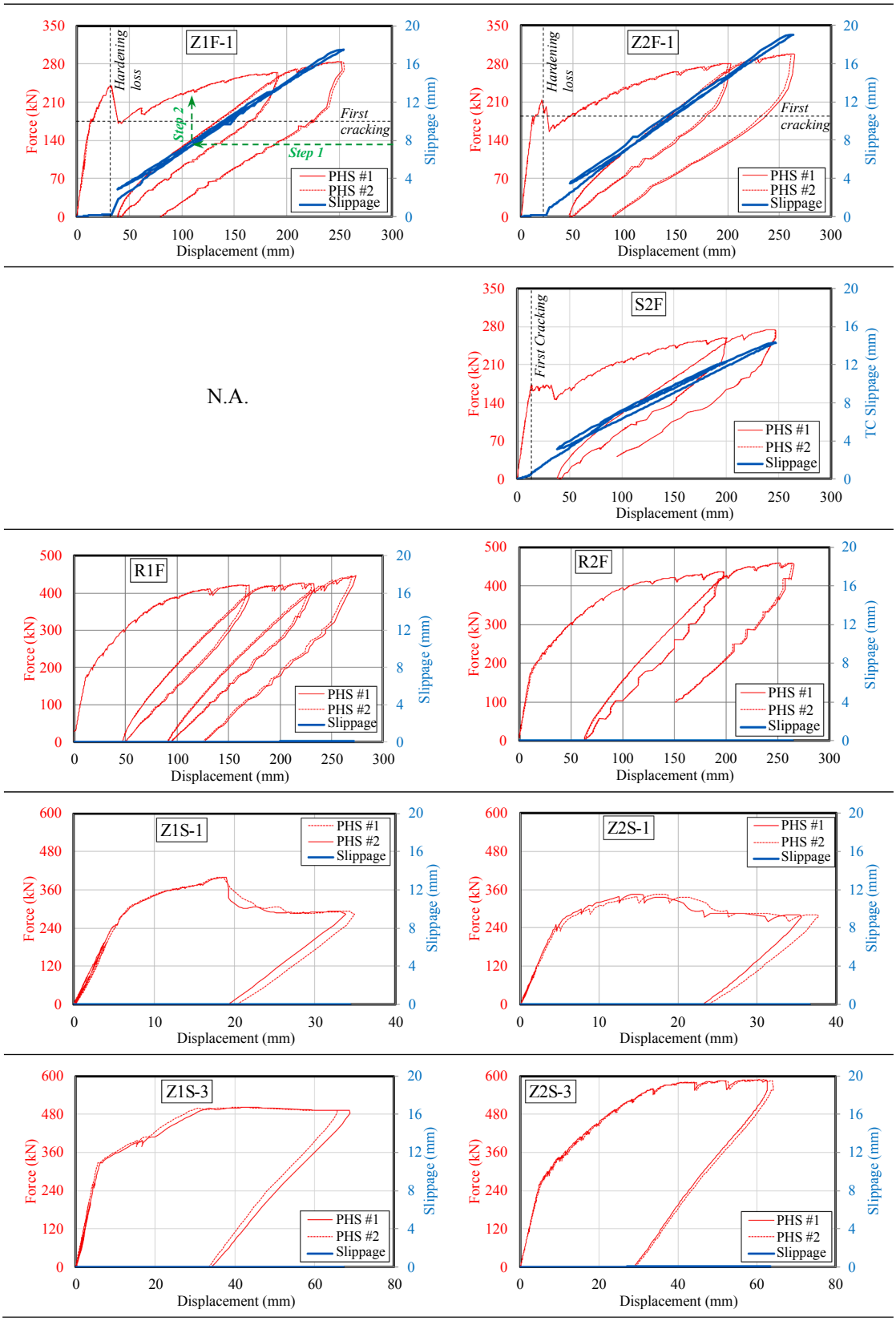

Fig. 8. Slippage between segments of the composite sections.

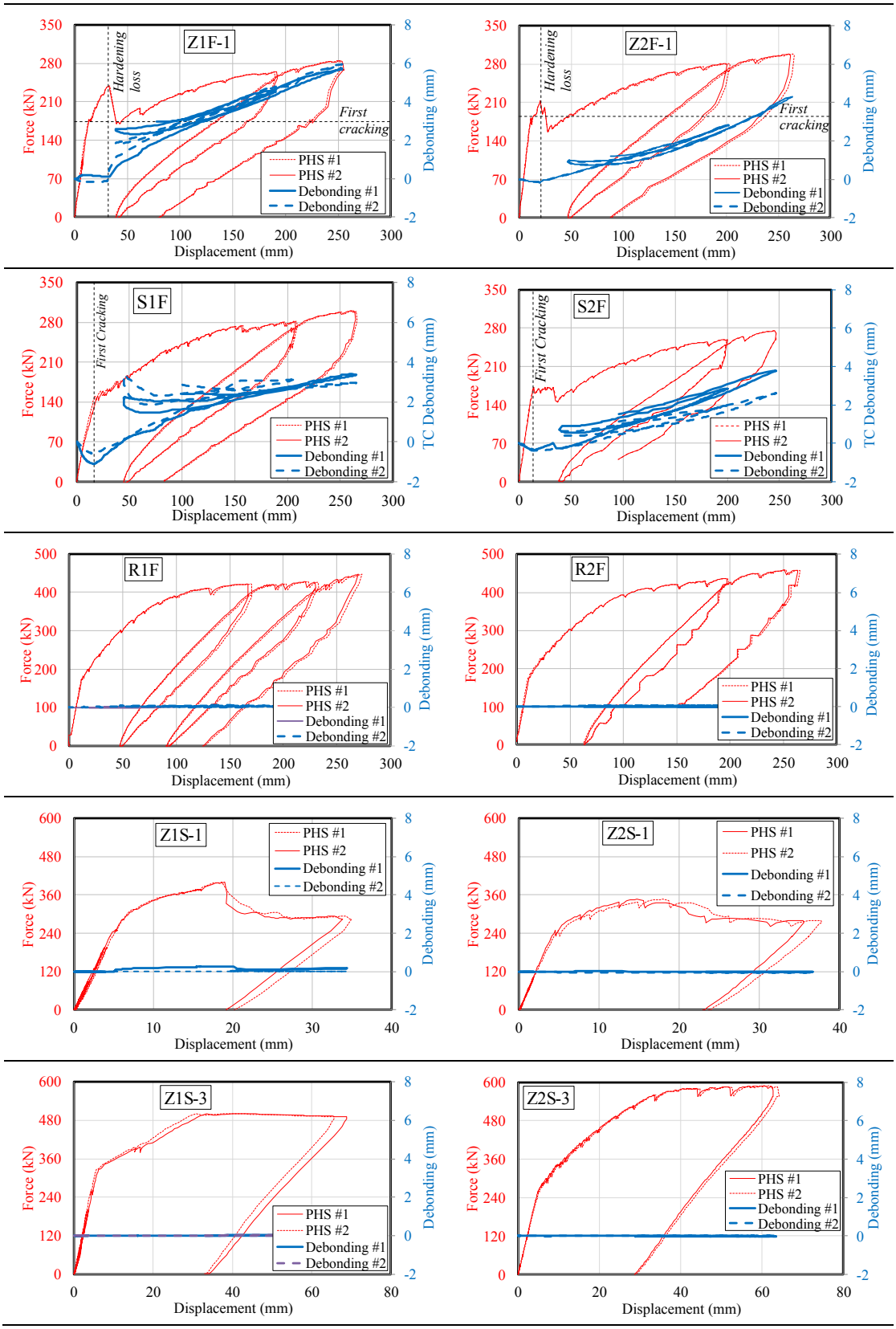

Fig. 9. Separation of segments of the composite sections.

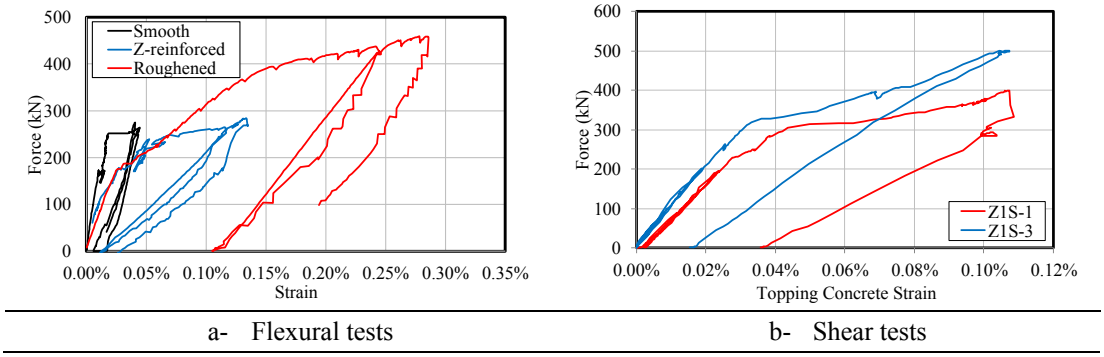

Fig. 10. Compressive strains at *TC*.

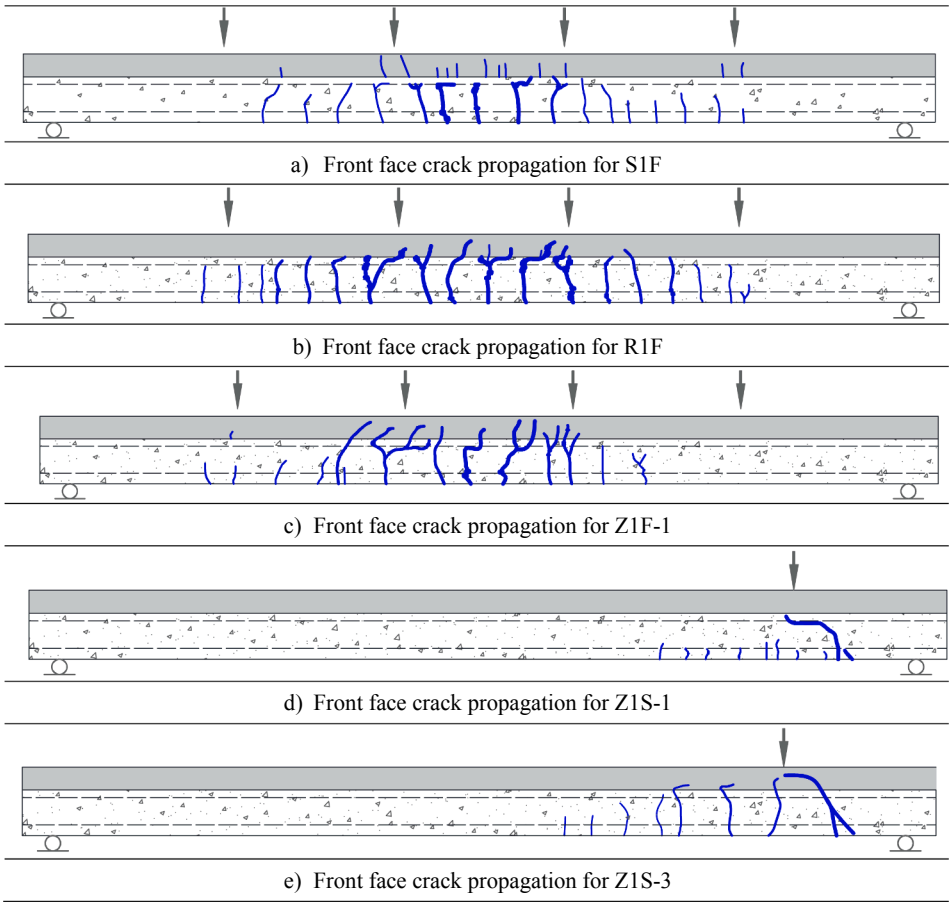

Fig. 11. Crack distributions at the ends of the tests.

various code estimations. The following conclusions can be made:

- Twins of full-scale specimens tested for the five diverse variables exhibited very similar behavior.
- All specimens had comparable initial stiffness till the first cracks occurred.
- The contribution of the Z-type shear connector utilized at the sole joint between *PHSs* is limited. After partial separation at the edges, the behavior was comparable with the smooth specimens.
- Full composite action was obtained for the roughened specimens and the specimens with three-row Z-type shear connectors (Z1S-3 and Z2S-3). The maximum interface shear stresses were 0.52 and 1.21 MPa.
- The placement of Z-type shear connectors at each longitudinal joint between *PHSs* will produce robust composite action.
- The maximum interface shear strength estimations of ACI 318M for the smooth specimens and the specimens with one-row Z-type shear connector (Z1F-1, Z2F-1, Z1S-1 and Z2S-1) were reasonable.
- The maximum interface shear strength estimations of ACI 318M for the roughened specimens and the specimens with three-row Z-type shear connectors (Z1S-3 and Z2S-3) were conservative.
- ACI-318 equations could be utilized to determine Z-type shear reinforcement area.
- A modification was proposed for the ACI 318M equation. The modified equation generates a reasonable estimation for the roughened specimens and the specimens with three-row Z-type shear connectors (Z1S-3 and Z2S-3).

a- Z1F-1 and Z2F-1

b- Smoot specimens

c- Roughened specimens

d- Z1S-1 and Z2S-1 e- Z1S-3 and Z2S-3

Fig. 12. The important damages observed from the specimens.

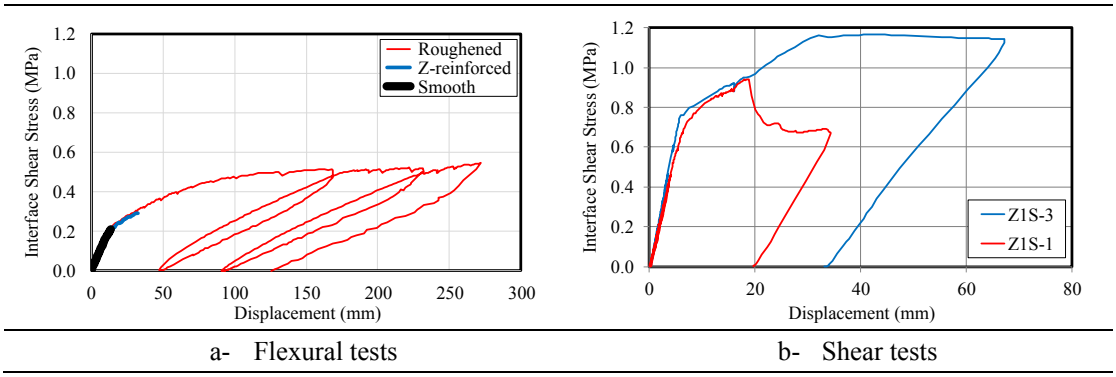

Fig. 13. Interface shear stresses.

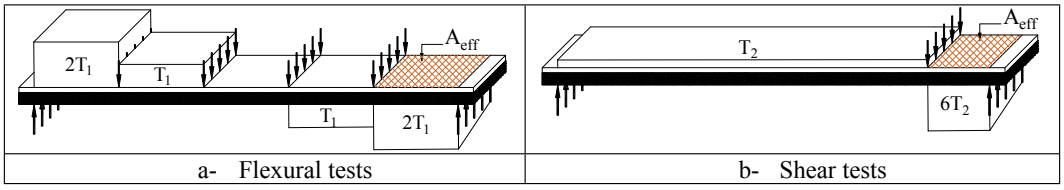

Fig. 14. Definition of effective shear area (A_{eff}).

Table 3
Horizontal shear stress estimations [MPa] of various codes.

Code	Equations	Specimen[1]	Flexural	Shear
ACI318-14	$T_i[N] = 0.55 b_w d$ $\tau_h[MPa] = T_i/A_{eff}$	S	×[2]	×
		R	0.393	×
		Z-1	×	×
		Z-3	×	0.550
EC-2 [4]	$V_{Rdi} = cf_{ctd} + \mu\sigma_n + \rho f_{yd}(\mu \sin\alpha + \cos\alpha) \leqslant 0.5\upsilon f_{cd}$ $\upsilon = 0.6\left(1 - \frac{f_{ck}}{250}\right)$ c = 0.2 and μ = 0.6 for smooth specimens c = 0.5 and μ = 0.9 for roughened specimens	S	0.304	×
		R	0.750	×
		Z-1	0.336	0.413
		Z-3	×	0.517
BS8110 [7]	0.600 MPa for smooth interfaces (C35) 0.775 MPa for roughened interfaces (C35)	S	0.600	×
		R	0.775	×
		Z-1	0.600	0.600
		Z-3	×	0.600
CEB-FIP	$\tau_u = c_r f_{ck}^{1/3} + \mu(\rho\kappa_1 f_{yd} + \sigma_n) + \kappa_2\rho\sqrt{f_{yd} f_{cd}} \leqslant \beta_c \upsilon f_{cd}$ All variables are defined in Randl [18].	S	0.010	×
		R	0.695	×
		Z-1	0.030	0.107
		Z-3	×	0.186
CSA [8]	$V_r = \phi_c\lambda(c + \mu\sigma_n) + \phi_s\frac{A_{vf}}{A_{cv}} f_{yd}\cos\alpha$ $\sigma_n = \frac{A_{vf}}{A_{cv}} f_{yd} sin\alpha + \frac{N}{A_{cv}}\phi_c = 0.65,\ \phi_s = 0.85,\ \lambda = 1$ c = 0.25 and μ = 0.6 for smooth specimens c = 0.5 and μ = 1.0 for roughened specimens	S	0.169	×
		R	0.352	×
		Z-1	0.194	0.246
		Z-3	×	0.326

[1] S smooth, R roughened, Z-1 one-row Z reinforced, Z-3 three-rows Z reinforced.
[2] Not Applicable.

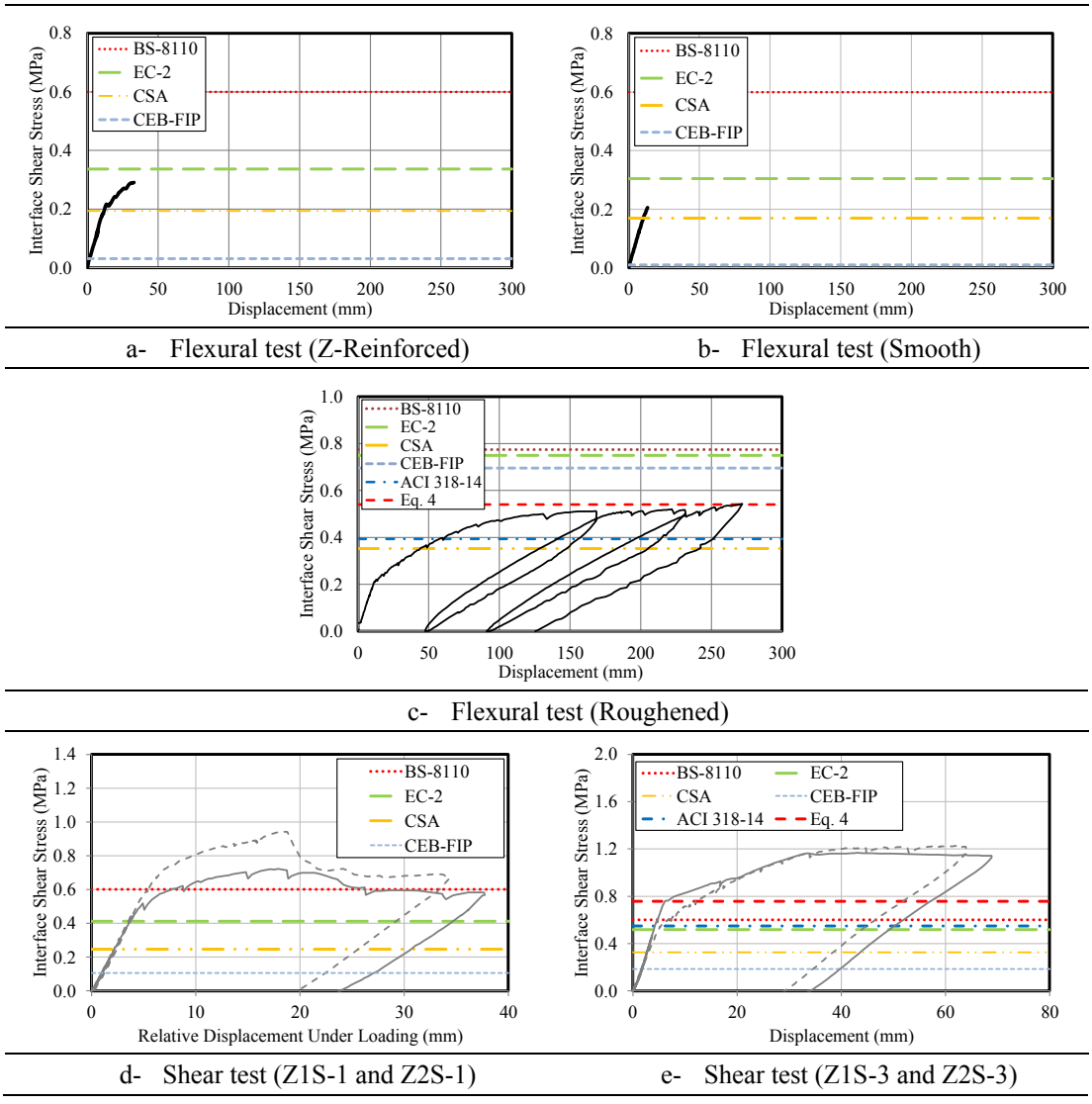

Fig. 15. Comparison of the code specified interface shear strength with the experiments.

Declaration of Competing Interest

The authors declare that they have no known competing financial interests or personal relationships that could have appeared to influence the work reported in this paper.

Acknowledgement

This study was conducted in the framework of İTÜNOVA Technology Transfer Office Research Project titled "*Evaluation of Interaction Between Hollow Core Slab and Topping Concrete*". The financial support provided by Turkish Precast Concrete Association through this project is greatly appreciated. The specimens were produced by Yapı Merkezi Prefabrikasyon A.Ş. and PB Prefabrik A.Ş. The study was conducted at the Structural and Earthquake Engineering Laboratory (STEELab) of Istanbul Technical University. Support from laboratory staff and the valuable contributions of Mr. Günkut Barka and Mr. Hakan Ataköy are gratefully acknowledged.

Appendix A. Supplementary material

Supplementary data to this article can be found online at https://doi.org/10.1016/j.engstruct.2020.110563.

References

[1] ACI (American Concrete Institute). Building code requirements for structural concrete. ACI 318M. Farmington Hills, MI: ACI; 2014.
[2] Adawi A, Youssef MA, Meshaly ME. Experimental investigation of the composite action between hollowcore slabs with machine-cast finish and concrete topping. Eng Struct. 2015;91:1–15.
[3] Ajdukiewicz A, Kliszczewicz A, Weglors M. Experimental study on the effectiveness of interaction between pre-tensioned hollow-core slabs and concrete topping. Archit Civ Eng Environ 2008;1:57–66.
[4] CEN. Eurocode 2: design of concrete structures – Part 1-1: general rules and rules for buildings: EN 1992-1-1. Brussels, European Committee for Standardization.
[5] Baran E. Effects of cast-in-place concrete topping on flexural response of precast concrete hollow-core slabs. Eng Struct. 2015;98:109–17.
[6] Bernardi P, Cerioni R, Leurini F, Michelini E. A design method for the prediction of load distribution in hollow core floors. Eng Struct. 2016;123:473–81.
[7] BSI. Structural use of concrete – Part 1: code of practice for design and construction: BS 8110-1. London, British Standard Institute.
[8] CAN/CSA A23.3. Design of concrete structures – structures design. Ontario, Canada: Canadian Standard Association; 2004.
[9] Federation international du beton (fib): model code 2010 final draft (2012). fib Bulletin No. 65/66, Lausanne.
[10] Girhammar UA, Pajari M. Tests and analyses on shear strength of composite slabs of hollow core units and concrete topping. Constr Build Mater. 2008;22:1708–22.
[11] Ibrahim IS, Elliott KS, Abdullah R, Kueh ABH, Sarbini NN. Experimental study on the shear behavior of precast concrete hollow core slabs with concrete topping. Eng Struct. 2016;125:80–90.
[12] Julio ENBS, Branco FAB, Silva VD. Concrete-to-concrete bond strength. Influence of the roughness of the substrate surface. Constr Build Mater. 2004;18:675–81.
[13] Loov RE, Patnaik AK. Horizontal shear strength of composite concrete beams with a

rough interface. PCI J. 1994;39(1):48–69.
[14] Mones RM, Brena SF. Hollow-core slabs with cast-in-place concrete toppings: a study o interfacial shear strength. PCI J. 2013;58(3):124–41.
[15] Pajari M, Koukkari H. Shear resistance of PHC slabs supported on beams I: tests. J Struct Eng 1998;124(9):1050–61.
[16] Pajari M. Shear resistance of PHC slabs supported on beams II: analysis. J Struct Eng 1998;124(9):1062–73.
[17] PCI Precast/Prestressed Concrete Institute. PCI design handbook: Precast and prestressed concrete, 7th ed. Chicago; 2010.
[18] Randl N. Design recommendations for interface shear transfer in *fib* model code 2010. Struct Concr 2013;14(3):230–41.
[19] Santos PMD, Julio ENBS. A state-of-the-art review on shear-friction. Eng Struct. 2012;45:435–48.
[20] Scott NL. Performance of precast prestressed hollow core slab with composite concrete topping. PCI J. 1973;18(2):64–77.
[21] Ueda T, Stitmannaithum B. Shear strength of precast prestressed hollow slabs with concrete topping. ACI Struct J 1991;88(4):402–10.
[22] Yang BL. Design of prestressed hollow core slabs with reference to web shear failure. J Struct Eng 1994;120(9):2675–96.